Inorganic Chemistry

Article

pubs.acs.org/IC

Synthesis, Structures, and Luminescent Properties of Uranyl Terpyridine Aromatic Carboxylate Coordination Polymers

Sonia G. Thangavelu,[†] Michael B. Andrews,[†] Simon J. A. Pope,[‡] and Christopher L. Cahill*[,†]

[†]Department of Chemistry, The George Washington University, 725 21st Street, NW, Washington, D.C. 20052, United States

[‡]School of Chemistry, Main Building, Cardiff University, Cardiff, Cymru/Wales, CF10 3AT U.K.

Supporting Information

ABSTRACT: Six novel uranyl terpyridine aromatic carboxylate coordination polymers, $[UO_2(C_6H_2O_4S)(C_{15}H_{11}N_3)]$ (**1**), $[UO_2(C_6H_2O_4S)(C_{15}H_{10}N_3Cl)]\cdot H_2O$ (**2**), $[UO_2(C_8H_4O_4)(C_{15}H_{11}N_3)]$ (**3**), $[UO_2(C_8H_4O_4)(C_{15}H_{10}N_3Cl)]$ (**4**), $[UO_2(C_{12}H_6O_4)(C_{15}H_{11}N_3)]$ (**5**), and $[UO_2(C_{12}H_6O_4)(C_{15}H_{10}N_3Cl)]$ (**6**), were synthesized under solvothermal conditions and characterized by single-crystal and powder X-ray diffraction and luminescence and UV−vis spectroscopy. Compounds **1**, **2**, and **5** crystallize as molecular uranyl dimers, whereas compounds **3**, **4**, and **6** contain ladder motifs of uranyl centers. Fluorescence spectra of **1**−**4** show characteristic UO_2^{2+} emission, wherein bathochromic and hypsochromic shifts are noted as a function of organic species. In contrast, uranyl emission from **5** and **6** is quenched by the naphthalene dicarboxylic acid linker molecules.

INTRODUCTION

Uranyl coordination polymers (CPs) synthesized using hydro(solvo)thermal techniques exhibit tremendous structural diversity owing, in part, to the tendency of the UO_2^{2+} cation to hydrolyze under such conditions. The resulting oligomeric species (or secondary building units) contribute to the structural diversity of uranyl bearing hybrid architectures. Indeed uranyl CPs consisting of monomers through octamers (as well as infinite sheets) have been well documented and continue to be a rich area of inquiry owing not only to this diverse speciation but also to the nearly limitless combinations of organic linkers.[1−9]

An inherent challenge to these syntheses, however, is directing speciation to a specific uranyl species of interest. One approach to simplifying aqueous reaction systems and effectively thwarting hydrolysis is to use high halide media wherein speciation is restricted to the $[UO_2X_4]^{2-}$ (X = Cl, Br) units almost exclusively.[1] The route to the formation of hybrid materials then becomes one of assembly of the tetrahalide anions using (for example) various organic cations.[10,11] This approach has been rather successful in producing a number of materials assembled through hydrogen-bonding and halogen−halogen interactions.

Another approach to offsetting the otherwise complex aqueous speciation of the uranyl cation is to use ligands that may show an affinity for a given building unit and effectively "select" a single species. As we have explored herein, chelating ligands such as terpyridines (TPYs) may prefer to coordinate to a single uranyl species and, consequently, impart a specific geometric arrangement to uranyl centers. From a crystal engineering perspective, this provides for coordination wherein TPY ligands may "lock" the metal center into place and allow for subsequent coordination at open binding sites on the other side of a metal "node" using multitopic linker molecules. Indeed, a number of uranyl terpyridine complexes have been reported and confirm either uranyl monomers[12,13] or, at most, dimers.[14,15]

Beyond the potential selectivity (and, indeed, structural rigidity) offered by TPYs, these ligands and other extended π systems may also contribute to the overall electronic properties of a material. For example, unique photophysical behavior may result as a consequence of $\pi-\pi^*$ transitions within the linkers or from energy transfer between metal centers and coordinated (or neighboring) organic species.[16] CPs containing lanthanide(III) ions are exemplary in this regard in that energy transfer from excited linker molecules or noncoordinated "guests" to emissive states with the lanthanide has been well documented.[16−19] Such are examples of sensitized emission, also known as the antenna effect, wherein nonradiative energy transfer commonly takes place from an excited ligand triplet state to excited state(s) on the lanthanide.[20,21] Requirements for promoting this energy transfer include a reasonable physical proximity between the organic chromophore and the emissive ion, as well as an appropriately matched energy level of the excited states on each. As such, thiophene-2,5-dicarboxylate (TDC),[22,23] benzene-1,4-dicarboxylate (BDC),[24,25] and naphthalene-1,4-dicarboxylate (NDC)[26] are known to be efficient sensitizing ligands for different lanthanide ions, and examples of uranyl CPs containing these and related ligands along with their luminescence have been reported.[27−33] TPYs also exhibit interesting luminescent properties and are useful for forming building blocks for the supramolecular assemblies of emissive lanthanide materials.[34,35]

Received: November 12, 2012
Published: January 31, 2013

 © 2013 American Chemical Society dx.doi.org/10.1021/ic3024698 | *Inorg. Chem.* 2013, 52, 2060−2069

Table 1. Crystallographic Data for Compounds 1−6

	1	2	3	4	5	6
formula	$[UO_2(C_6H_2O_4S)(C_{15}H_{11}N_3)]$	$[UO_2(C_6H_2O_4S)(C_{15}H_{10}N_3Cl)]\cdot H_2O$	$[UO_2(C_8H_4O_4)(C_{15}H_{11}N_3)]$	$[UO_2(C_8H_4O_4)(C_{15}H_{10}N_3Cl)]$	$[UO_2(C_{12}H_6O_4)(C_{15}H_{11}N_3)]$	$[UO_2(C_{12}H_6O_4)(C_{15}H_{10}N_3Cl)]$
fw	673.44	725.91	667.41	701.86	717.47	751.92
temperature (K)	100	100	293	100	100	300
wavelength (Å)	0.71073	0.71073	0.71073	0.71073	0.71073	0.71073
cryst syst	monoclinic	monoclinic	monoclinic	monoclinic	triclinic	monoclinic
space group	$P2_1/n$	$P2_1/c$	$C2/c$	$C2/c$	$P\bar{1}$	$P2_1/c$
unit cell dimens						
a (Å)	9.5824(3)	11.0786(16)	13.011(5)	12.486(3)	8.9758(7)	10.6869(13)
b (Å)	13.5216(5)	12.1200(18)	15.901(5)	14.736(3)	11.3079(8)	8.3588(9)
c (Å)	16.2164(5)	16.164(2)	11.739(5)	12.268(3)	12.2348(9)	26.656(4)
α (deg)					78.4550(10)	
β (deg)	102.0320(10)	97.958(2)	118.035(5)	113.494(2)	81.2450(10)	92.075(4)
γ (deg)					67.1190(10)	
volume (Å^3)	2054.99(12)	2149.4(5)	2143.7(14)	2070.1(8)	1117.13(14)	2379.6(5)
Z	4	4	4	4	2	4
density (calcd) (Mg/m^3)	2.170	2.184	2.068	2.265	2.133	2.054
abs coeff (mm^{-1})	8.046	7.818	7.618	8.023	7.318	6.983
reflns collected	40347	34042	6665	8545	21319	14646
indep reflns	5938 [R(int) = 0.0810]	4707 [R(int) = 0.0886]	1887 [R(int) = 0.0384]	2207 [R(int) = 0.0437]	6015 [R(int) = 0.0302]	4176 [R(int) = 0.0989]
final R indices [$I > 2\sigma(I)$]	R1 = 0.0359, wR2 = 0.0889	R1 = 0.0405, wR2 = 0.1012	R1 = 0.0208, wR2 = 0.0509	R1 = 0.0251, wR2 = 0.0499	R1 = 0.0351, wR2 = 0.0822	R1 = 0.0421, wR2 = 0.1025

The emissive properties of the uranyl cation have been known for some time and, consequently, studied extensively from a fundamental perspective as well as from a more analytical and applied approach as relevant to (for example) environmental investigations of uranyl speciation.[36−38] Despite this interest, studies of uranyl emission from within hybrid materials have been a bit less frequent and more qualitative in nature, even considering the potential for these compounds to serve as photocatalysts.[8,39,40] An inherent challenge to studying energy transfer between linker and uranyl centers is the overlap of the $\pi-\pi^*$ absorption of the organic linkers in UV−vis and ligand-to-metal charge-transfer (LMCT) absorption within the UO_2^{2+} itself. As a consequence, one cannot completely resolve the contribution from the linker(s) or UO_2^{2+} without thorough quantitative analysis and modeling efforts. Indeed some of our own earlier studies were highly qualitative and speculative with respect to UO_2^{2+} sensitization.[41,42] The continued development of hybrid materials particularly using the approaches described herein may contribute to a platform for accessing materials that allow for a more systematic study of the photophysical properties. As such, this contribution reports the synthesis of six uranyl terpyridine dicarboxylate CPs that have been characterized by single-crystal and powder X-ray diffraction, luminescence, and UV−vis spectroscopy in which we demonstrate that uranyl emission may be influenced as a function of coordinated aromatic carboxylate and TPY ligands.

EXPERIMENTAL SECTION

General Synthesis of Compounds 1−6. All starting materials were purchased from VWR except TDC (Sigma Aldrich) and used as received without further purification.

Caution! *Uranyl acetate, $UO_2(CH_3COO)_2\cdot 2H_2O$, contains depleted uranium. Standard operating procedures for the handling of radioactive and toxic substances should be followed.*

All compounds were synthesized according to the following general procedure with the same molar ratio of reactants. A mixture of uranyl acetate (1.0 equiv, 0.251 mmol), organic acid (1.5 equiv, 0.377 mmol), TPY (1.5 equiv, 0.377 mmol), and 25 μL of 6 M NaOH was dissolved in 2.5 mL of a H_2O−2-propanol (1:1.5) mixture. All reagents were placed in a 23 mL Teflon-lined stainless steel Parr bomb, which was sealed and heated statically for 5 days at 120 °C. The Parr bomb was then allowed to cool slowly to 25 °C overnight. Solids were collected, washed with H_2O and 2-propanol, and allowed to air-dry. Single crystals were then isolated and characterized by single-crystal X-ray diffraction (XRD). Elemental analyses were performed on all products by Galbraith Laboratories, Knoxville, TN. Syntheses of **1−6** were also performed in deionized H_2O (2.5 mL) yet yielded impure reaction products, as evidenced by powder X-ray diffraction (PXRD; see Figures S18−S23 in the Supporting Information).

*$[UO_2(C_6H_2O_4S)(C_{15}H_{11}N_3)]$ (**1**).* Yellow block crystals using TDC and TPY. Yield: 116.0 mg, 69% based on uranium. Elem anal. Obsd (calcd): C, 37.32 (37.42); H, 1.95 (1.95); N, 5.50 (6.24).

*$[UO_2(C_6H_2O_4S)(C_{15}H_{10}N_3Cl)]\cdot H_2O$ (**2**).* Yellow block crystals using TDC and Cl-TPY. Yield: 131.6 mg, 72% based on uranium. Elem anal. Obsd (calcd): C, 34.74 (35.68); H, 1.94 (1.71); N, 5.79 (5.94).

*$[UO_2(C_8H_4O_4)(C_{15}H_{11}N_3)]$ (**3**).* Yellow block crystals using BDC and TPY. Yield: 143.6 mg, 86% based on uranium. Elem anal. Obsd (calcd): C, 41.76 (41.39); H, 2.42 (2.27); N, 5.60 (6.30).

*$[UO_2(C_8H_4O_4)(C_{15}H_{10}N_3Cl)]$ (**4**).* Yellow block crystals using BDC and Cl-TPY. Yield: 91.7 mg, 52% based on uranium. Elem anal. Obsd (calcd): C, 39.09 (39.32); H, 2.11 (2.01); N, 5.81 (5.98).

*$[UO_2(C_{12}H_6O_4)(C_{15}H_{11}N_3)]$ (**5**).* Yellow block crystals using NDC and TPY. Yield: 158.2 mg, 87% based on uranium. Elem anal. Obsd (calcd): C, 45.16 (44.95); H, 2.42 (2.37); N, 5.70 (5.85).

*$[UO_2(C_{12}H_6O_4)(C_{15}H_{10}N_3Cl)]$ (**6**).* Yellow block crystals using NDC and Cl-TPY. Yield: 86.2 mg, 47% based on uranium. Elem anal. Obsd (calcd): C, 45.38 (43.09); H, 2.13 (2.19); N, 5.71 (5.59).

PXRD. Diffraction patterns of compounds **1−6** were obtained on a Rigaku MiniFlex II Desktop powder X-ray diffractometer (Cu Kα, 3−60°) and analyzed using the *JADE* software package. The phase purity of bulk samples **1−6** was assessed by a comparison of the observed and calculated PXRD patterns. These patterns can be found in the Supporting Information (Figures S1−S6). Compound **6** required washing of the bulk sample with chloroform, in addition to H_2O and 2-propanol, to achieve phase purity.

UV−Vis and Fluorescence Measurements. Solid-state UV−vis diffuse-reflectance spectra were recorded on a Jasco V-570 UV−vis−

dx.doi.org/10.1021/ic3024698 | Inorg. Chem. 2013, 52, 2060−2069

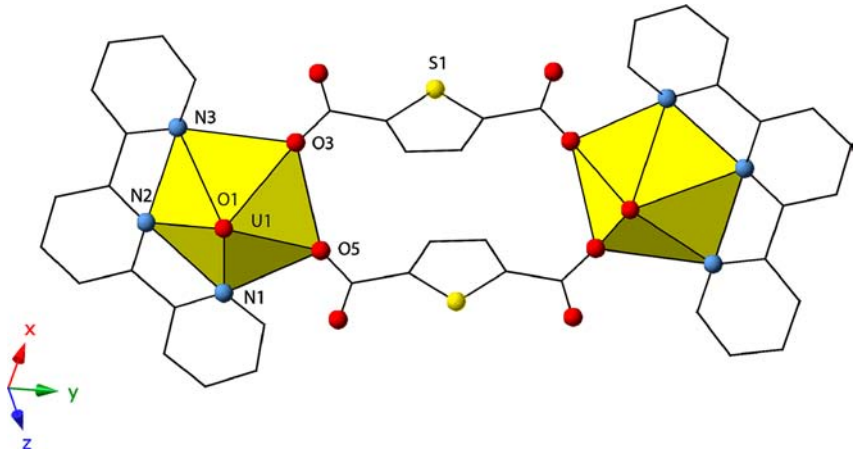

Figure 1. Molecular dimer found in **1**. Yellow polyhedra are uranyl centers, whereas spheres represent nitrogen (blue), oxygen (red), and sulfur (yellow).

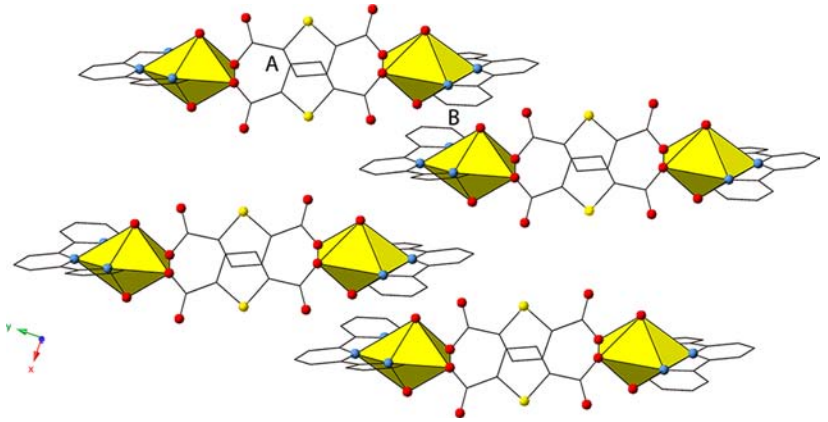

Figure 2. Packing diagram of **1** showing $\pi-\pi$ interactions of the thiophene rings (A) and outer pyridine rings of TPY (B) viewed along [001].

near-IR spectrophotometer equipped with an ISN-470 integrating sphere reflectance accessory at 298 K. These spectra can be found in the Supporting Information (Figure S13). Solid-state emission spectra of **1**–**6** and uranyl acetate were recorded on a Shimadzu RF-5301 spectrofluorophotometer at 298 K. All fluorescence spectra were collected with a 1.5 nm slit width for both excitation and emission monochromators, respectively, with the excitation wavelength fixed to 365 nm and are uncorrected.

Phosphorescence Measurements. To determine the triplet states of TDC and NDC, the following experiments were performed using Gd^{3+} to enhance the triplet yield of the ligand. A mixture of $Gd(NO_3)_3{\cdot}6H_2O$ (34 mg, 0.077 mmol, 1 equiv) and NDC (50 mg, 0.231 mmol, 3 equiv) or TDC (39.8 mg, 0.231 mmol, 3 equiv) was dissolved in 5 mL of a 1:9 MeOH–EtOH mixture in a 25 mL scintillation vial. The solution was gently heated to 50 °C to ensure complete dissolution of all materials. Control experiments for NDC and TDC were also prepared using the same molar ratios and solvents without Gd^{3+}. An aliquot of all prepared solutions was used as the glass matrix (i.e., 1:9 MeOH–EtOH) for spectral measurements at low temperature. Phosphorescence measurements were taken on a Horiba JobinYvon Fluorolog-3 spectrophotometer equipped with a liquid-nitrogen dewar assembly and a pulsed-UV xenon flash lamp at 77 K. Spectra were recorded under the right angle setting using a time delay of 5 ms to remove any residual fluorescence with the following parameters: the total cycle time per flash, sample window, and number of pulsed flashes were fixed to 61 ms, 0.2 ms, and 100, respectively. All phosphorescence spectra were collected with a slit width of 5 nm for both excitation and emission monochromators, respectively, with the excitation wavelength fixed to 320 nm, and are uncorrected. These spectra can be found in the Supporting Information (Figures S14–S17).

Crystal Structure Determination. Single crystals isolated from each bulk sample were mounted on MiTeGen micromounts. For structure determinations of **1**, **2**, and **5**, reflections were collected using 0.5° φ and ω scans on a Bruker SMART diffractometer equipped with an APEX II CCD detector using Mo Kα radiation. For structure determinations of **3** and **6**, reflections were collected using 0.5 φ scans on a Bruker SMART X2S benchtop diffractometer using Mo Kα radiation. For structure determination of **4**, reflections were collected on a Siemens SMART 1000 CCD three-circle X-ray diffractometer equipped with a LT-2 low-temperature apparatus using Mo Kα radiation. All data was integrated using the *SAINT* software package, and an absorption correction was applied using *SADABS*. All structures were solved using direct methods (*SHELXS-97*) and refined using *SHELXL-97* within the *WinGX* software package,[43,44] in which all of the non-hydrogen atoms were refined anisotropically with satisfactory refinements. Tests for additional symmetry were done using *PLATON*. A summary of the crystallographic data for **1**–**6** can be found in Table 1.

RESULTS AND DISCUSSION

Structural Description. *Crystal Structure of 1.* The crystal structures of **1**–**6** each exhibit a uranium(VI) center bound to two axial oxygen atoms at bond lengths between 1.763(3) and 1.784(4) Å and a O–U–O bond angle that ranges from 175.25(18)° to 178.26(17)°. These values are consistent with the characteristic bond distances and bond angles of the UO_2^{2+} cation.[45] The uranyl center of **1** (Figure 1) is bound

dx.doi.org/10.1021/ic3024698 | *Inorg. Chem.* 2013, 52, 2060–2069

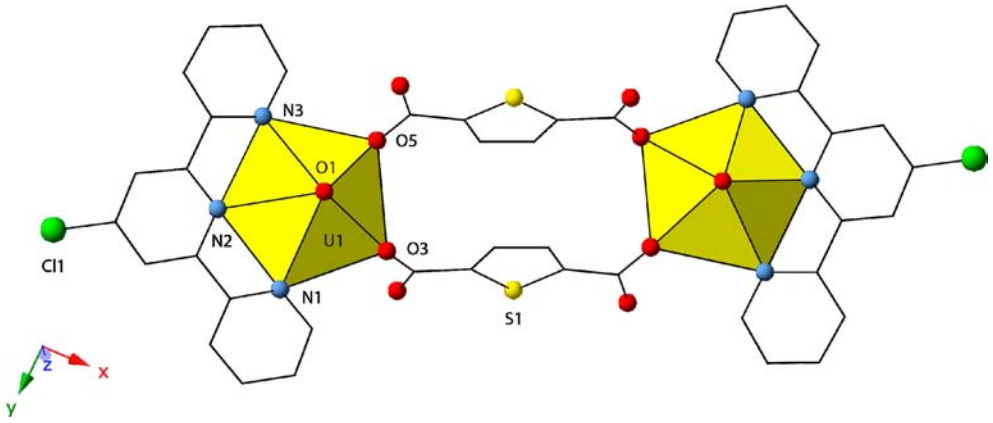

Figure 3. Molecular dimer found in **2**. The green spheres are chlorine atoms. H_2O is not shown for clarity.

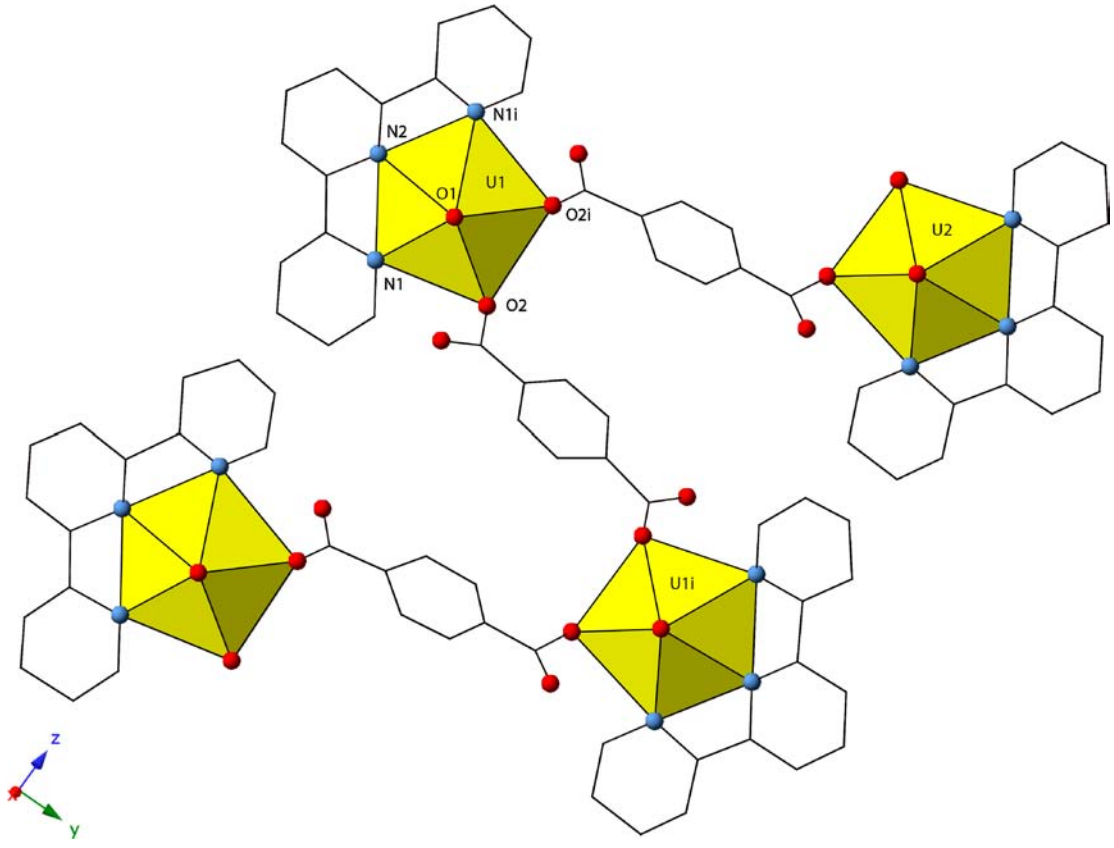

Figure 4. Extended structure of **3**. The subscript i represents the symmetry transformation $-x + 1, y, -z + {}^{1}/_{2}$.

equatorially to one TPY and two distinct monodentate TDC ligands to form an overall distorted pentagonal-bipyramidal geometry. Each TDC linker is bound to two uranyl centers through carboxylate oxygen atoms O3 and O5 at distances of 2.278(3) and 2.286(3) Å, respectively. The nonbonded carboxylate oxygen atoms O4 and O6 at distances of 1.225(6) and 1.223(5) Å, respectively, were identified as carbonyl oxygen atoms, which is in agreement to a C−O double bond distance of 1.20−1.25 Å.[46] For TPY, each nitrogen atom N1, N2, and N3 is bound to uranium at an average distance of 2.583(3) Å. The N1−U−N2 and O3−U−O5 bond angles formed by either TPY or each TDC linker were found to be 63.19(10)° and 80.03(10)°, respectively. The uranium metal centers are linked together by two bridging thiophenedicarboxylates to form discrete molecular dimers oriented along [010] (Figure 2), where the outer pyridines π-stack above and below each dimer at a ring centroid−centroid distance of 3.919(3) Å (A) as determined in *PLATON*. The bridging thiophene linkers also show $\pi-\pi$ interactions at a ring centroid−centroid distance of 3.661(2) Å (B). These values are in agreement with typical π-stacking distances of 3.3−3.8 Å for metal−aromatic complexes.[47]

Crystal Structure of ***2***. The uranyl center of **2** (Figure 3) is bound equatorially to Cl-TPY and two distinct TDC ligands to form an overall pentagonal-bipyramidal geometry. As in **1**, each TDC linker is bound to two uranyl centers through carboxylate oxygen atoms O3 and O5 at bond distances of 2.256(4) and 2.303(4) Å, respectively. Tridentate coordination by the nitrogen atoms N1, N2, and N3 in Cl-TPY to uranium shows an average bond distance of 2.590(5) Å. The nonbonded

dx.doi.org/10.1021/ic3024698 | *Inorg. Chem.* 2013, 52, 2060−2069

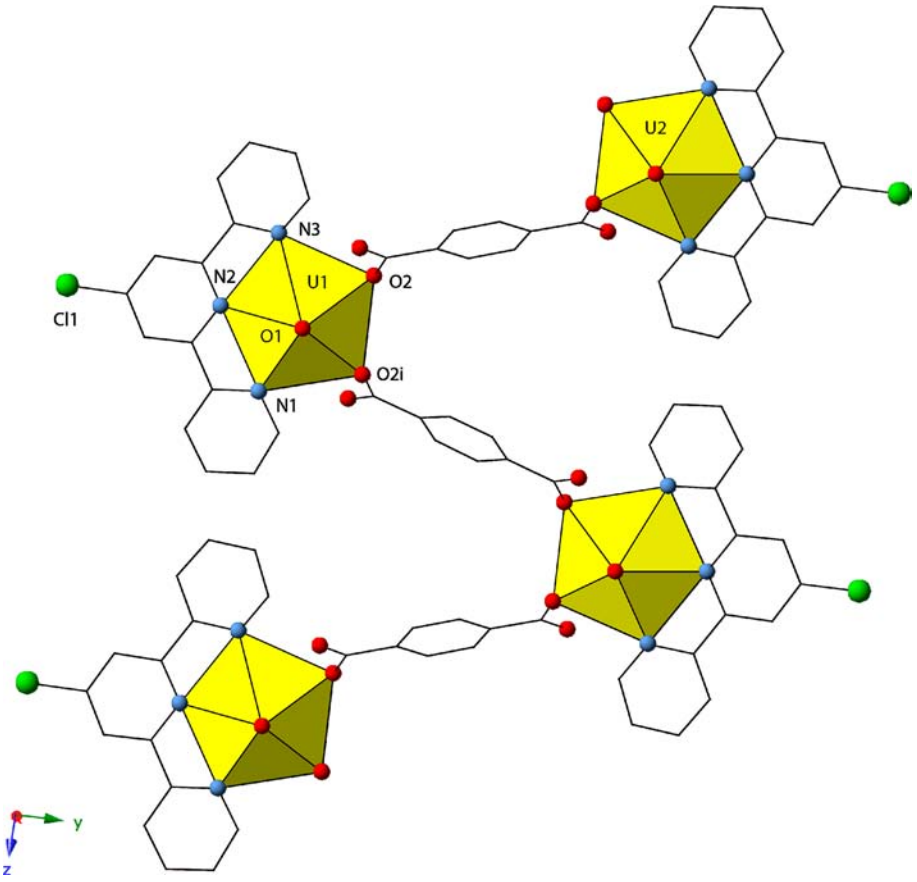

Figure 5. Portion of the extended structure of **4**.

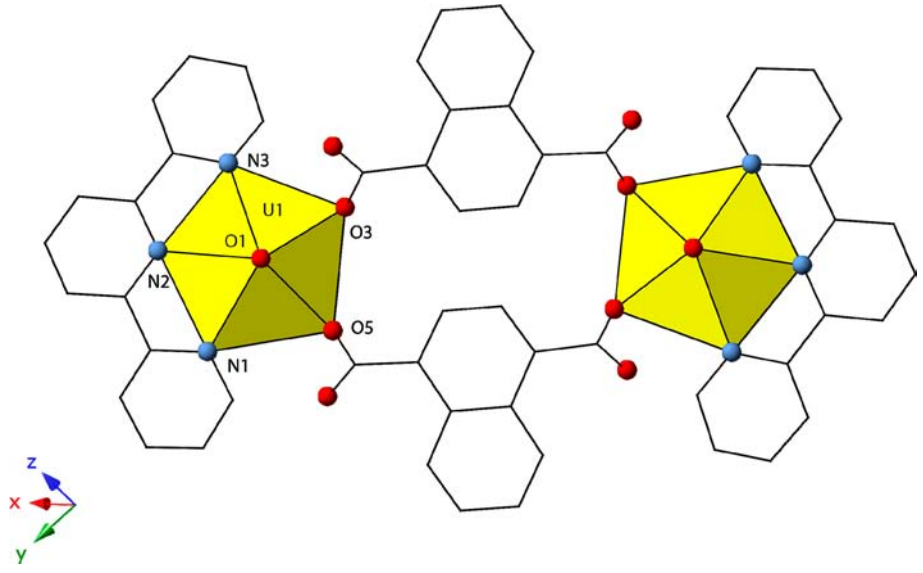

Figure 6. Molecular dimer found in **5**.

oxygen atoms O4 and O6 at distances of 1.213(7) and 1.225(8) Å, respectively, were identified as carbonyl oxygen atoms. The N1−U−N2 and O3−U−O5 equatorial bond angles formed by Cl-TPY and TDC was found to be 62.79(16)° and 79.75(15)°, respectively. Like **1**, each uranium atom is linked together by bridging thiophenecarboxylates in a monodentate fashion to form an overall molecular dimer (Figure 3) with an analogous packing arrangement. The bridging thiophene linkers, like those in **1**, show $\pi-\pi$ interactions at a ring centroid−centroid distance of 3.684(6) Å, yet the outer pyridine distance of Cl-TPY is 8.279(7) Å.

Crystal Structure of ***3***. Two crystallographically distinct uranyl centers, U1 and U2, are bound by two BDC linkers and one TPY, which have pentagonal-bipyramidal geometries (Figure 4). The BDC linkers are bound to uranyl by monodentate coordination through the carboxylate oxygen

dx.doi.org/10.1021/ic3024698 | *Inorg. Chem.* 2013, 52, 2060−2069

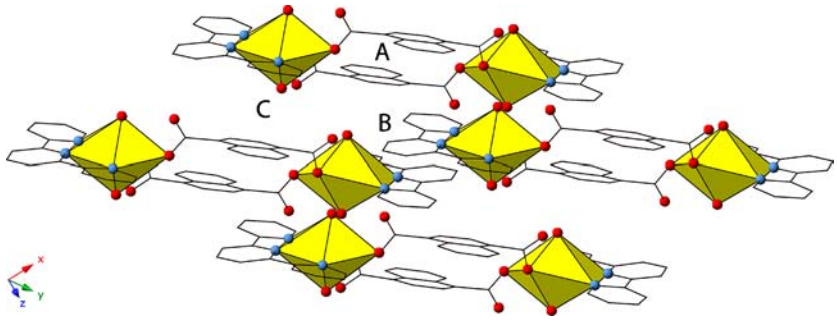

Figure 7. Packing diagram of **5** showing $\pi-\pi$ interactions of the naphthalene (A) and outer pyridine rings (B) of TPY and between the outer rings of TPY and naphthalene (C).

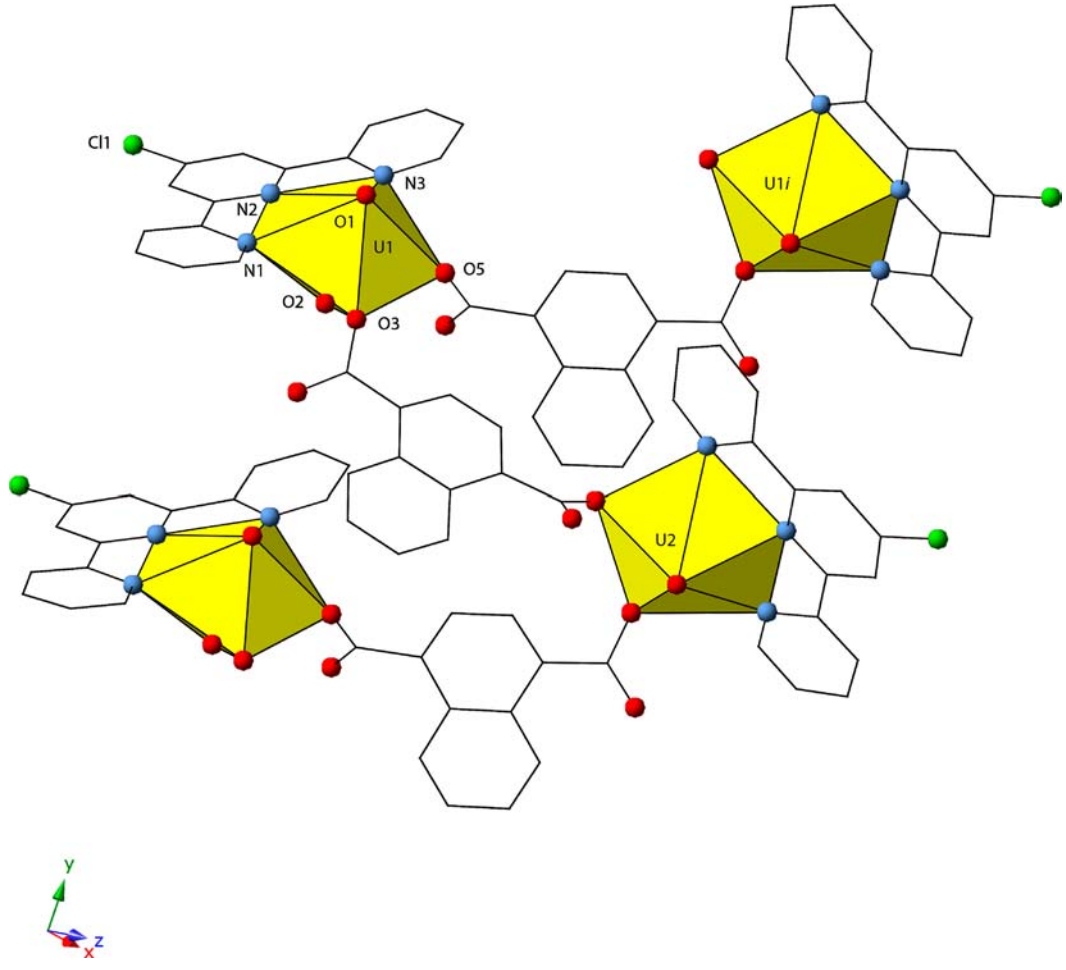

Figure 8. Extended structure of **6**.

atoms O2 and O2i with a bond length of 2.292(3) Å. Tridentate coordination through nitrogen atoms N1 and N2 of TPY to the uranyl center illustrates an average bond distance of 2.593(4) Å. Nonbonded oxygen atoms O3 and O3i at a bond length of 1.223(5) Å were identified as carbonyl oxygen atoms. Bond angles of N1−U−N2 and O2−U−O2i formed by TPY and BDC were found to be 63.01(7)° and 80.60(13)°, respectively, which are similar to the bond angles of **1** at 63.19(10)° and 80.03(10)°, respectively. Unlike the dimeric uranyl species found in **1** and **2**, the overall structure of **3** shows a "ladder motif" that propagates along [001] wherein uranyl terpyridine monomers are connected through BDC groups.

Crystal Structure of 4. The local geometry of the uranyl center U1 in **4** is a pentagonal bipyramid with equatorially bound Cl-TPY and BDC linkers. Like **3**, each BDC ligand is linked to two crystallographically distinct uranyl centers U1 and U2 (Figure 5). The BDC linker is coordinated to the uranium through a carboxylate oxygen atom O2 in a monodentate fashion at a bond distance of 2.303(3) Å. For Cl-TPY, the nitrogen atoms N1 and N2 are coordinated to the uranyl center with an average bond distance of 2.605(4) Å. The nonbonded oxygen atoms O3 and O3i at a bond length of 1.227(5) Å were identified as carbonyl oxygen atoms. The N1−U−N2 and O2−U−O2i bond angles formed by TPY and BDC are 62.87(8)° and 81.74(14)°, respectively. In addition, the N1−U−N2 and

dx.doi.org/10.1021/ic3024698 | *Inorg. Chem.* 2013, 52, 2060−2069

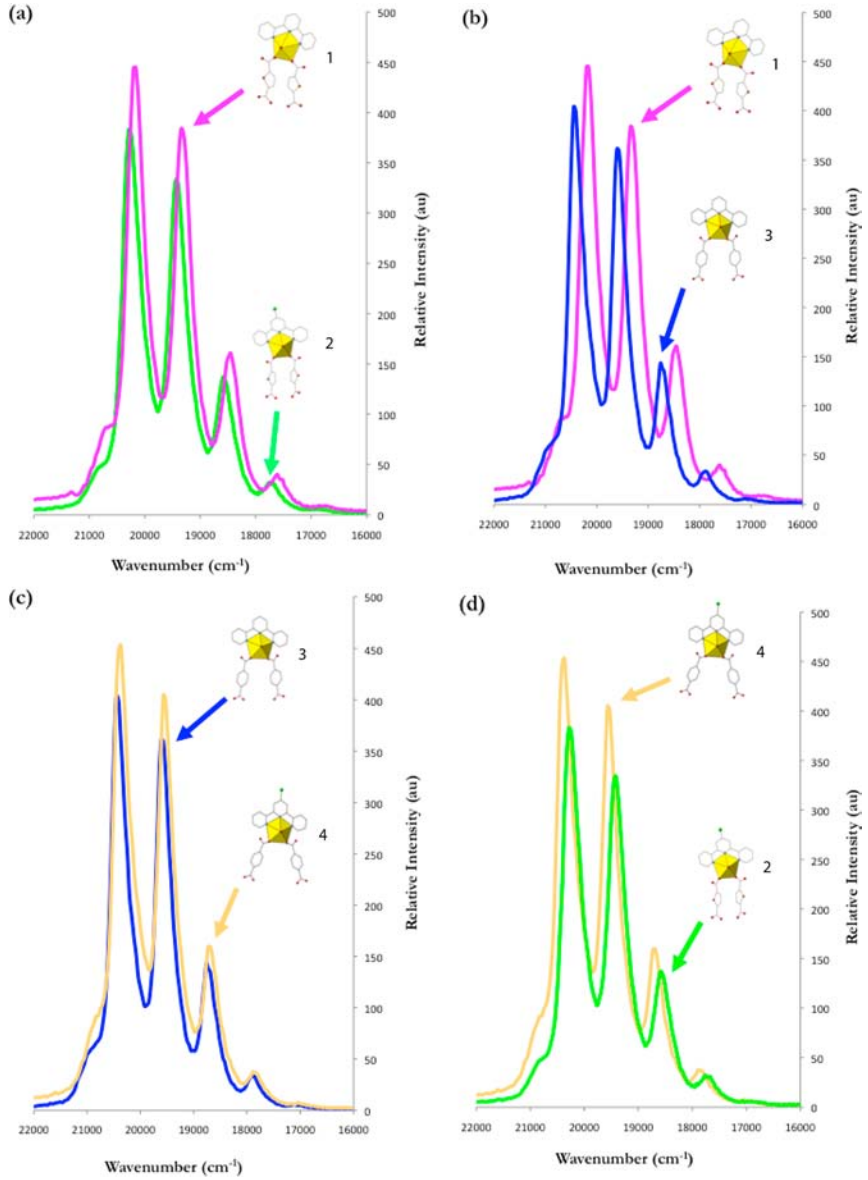

Figure 9. Solid-state emission spectra of **1**–**4** excited at 365 nm at room temperature: (a) comparison of **1** and **2**; (b) comparison of **1** and **3**; (c) comparison of **3** and **4**; (d) comparison of **2** and **4**.

O2–U–O2i bond angles of **4** are similar to **3** at 63.01(7)° and 80.60(13)°, respectively. Like **3**, the overall structure of **4** contains a ladder motif that propagates along [001].

*Crystal Structure of **5**.* The crystal structure of **5** shows an overall pentagonal-bipyramidal geometry of the uranium metal center bound by two distinct NDC linkers and one TPY (Figure 6). Like **1** and **2**, the oxygen atoms O3 and O5 of NDC are coordinated to the metal in a monodentate fashion, exhibiting bond distances of 2.303(6) and 2.280(6) Å, respectively. For TPY, coordination through the nitrogen atoms N1, N2, and N3 shows an average bond distance of 2.589(7) Å. The nonbonded oxygen atoms O4 and O6 at bond lengths of 1.223(10) and 1.211(10) Å, respectively, were identified as carbonyl oxygen atoms. The N1–U–N2 and O3–U–O5 bond angles formed by NDC and TPY are 63.15(2)° and 80.61(2)°, similar to the bond angles of **1**–**4**. The uranium metal centers are linked together by bridging NDC carboxylate groups to form a molecular dimer of **5**, as seen previously for **1** and **2**. These dimers are then oriented along the [110] direction to form the overall extended structure (Figure 7). Three types of π-stacking arrangements are observed in the molecular packing. First, two bridging naphthalene rings show π–π interaction with each other at a ring centroid C–H distance of 3.618(5) Å (A). This is consistent with the reported π stacking of naphthalene rings for uranyl NDC CPs at distances of 3.3–3.45 Å,[5,25] suggesting that π–π interactions for **5** are comparable and within the acceptable range of π-stacking distances.[47] Another π–π interaction is observed between the outer pyridine rings, which stack above and below each dimer at a ring centroid–centroid distance of 3.651(5) Å (B). Lastly, π stacking is also present between the naphthalene and outer pyridine rings of adjacent dimers with a ring centroid–centroid distance of 3.580(5) Å (C).

*Crystal Structure of **6**.* The uranyl center of **6** is bound equatorially to two distinct NDC linkers and one Cl-TPY to form an overall pentagonal-bipyramidal geometry. Similarly to **3** and **4**, each NDC linker is bound to two distinct uranyl centers (Figure 8). The oxygen atoms O3 and O5 of NDC are

dx.doi.org/10.1021/ic3024698 | *Inorg. Chem.* 2013, 52, 2060–2069

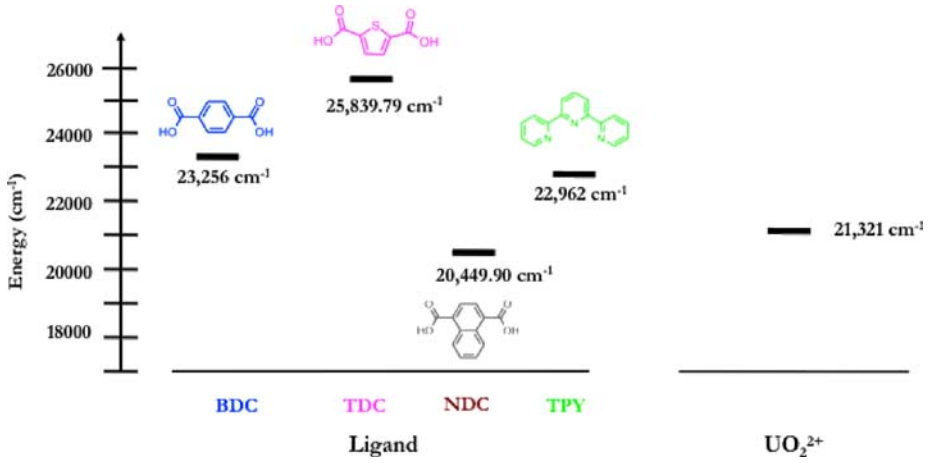

Figure 10. Diagram of the energy levels of ligand triplet states (77 K) and the highest excited state of UO_2^{2+} (298 K).

coordinated to the uranyl center in a monodentate fashion at distances of 2.257(7) and 2.312(7) Å, respectively. For Cl-TPY, the nitrogen atoms N1, N2, and N3 are coordinated to the uranyl center at an average distance of 2.585(8) Å. The nonbonded carboxylate oxygen atoms O4 and O6 at distances of 1.222(12) and 1.229(12) Å, respectively, were identified as carbonyl oxygen atoms. The N1−U−N2 and O3−U−O5 bond angles formed by either Cl-TPY or each NDC linker were found to be 62.72(3)° and 83.61(3)°. Like **3** and **4**, the uranyl centers in **6** are linked together by NDC carboxylate groups as a ladder motif propagating roughly along [101].

Synthesis. The syntheses of **1**−**6** were carried out under solvothermal reaction conditions in a H_2O−2-propanol mixture at 120 °C for 5 days. The initial pH was adjusted between 5.2 and 5.8 using 6 M NaOH, which resulted in crystals suitable for single-crystal XRD. Different structures were observed as either uranyl dimers (**1**, **2**, and **5**) or ladder motifs (**3**, **4**, and **6**) of the uranyl centers. It is worth noting that the uranyl cation exists as a monomer in **1**−**6** considering the tendency of this moiety to hydrolyze in this pH range.[2,38] A possible explanation of why we do not observe oligomers in our system may be attributed to the role of sterics and choice of ligands, which may influence uranyl hydrolysis. One may speculate that the presence of TPY ligands prevents uranyl hydrolysis because the steric contribution of the aromatic groups may reduce the number of available open coordination sites necessary to promote oligomerization. The reasons for the different structural types for **1**−**6** can be explained as a function of the aromatic linker and substituent on the TPY ligand. When TDC linkers are used, dimers are observed (**1** and **2**), whereas the use of BDC results in ladder motifs (**3** and **4**). This may be due to the size of the aromatic ring (i.e., five-membered thiophene versus six-membered benzene), which results in different structural motifs. For the NDC ligand, however, the steric argument is not a clear indication of why we observe both dimer and ladder motifs (**5** and **6**) and may point to more complex packing considerations between TPY and Cl-TPY.

Fluorescence Studies. The origin of UO_2^{2+} emission is caused by electronic transitions between the lowest unoccupied molecular orbital (LUMO) $5f_\delta$ and $5f_\varphi$ nonbonding uranium(VI) orbitals and the highest occupied molecular orbital (HOMO) 6d−5f−2p U−O $3\sigma_u$ bond.[48] Within these spectra, six distinct peaks between 470 and 590 nm are observed, which represent the vibronic structure of the uranyl cation caused by symmetric and antisymmetric oscillations within the U−O bond.[49,50] The solid-state emission spectra of **1**−**4** obtained at an excitation wavelength of 365 nm show uranyl emission (Figure 9), and additional spectroscopic features of UO_2^{2+} can be found in its UV−vis diffuse-reflectance spectrum (see Figure S13 in the Supporting Information). The UV component corresponds to the LMCT transitions from the HOMO U−O bond to the LUMO nonbonding uranium(VI) orbitals, whereas the visible component corresponds to the LMCT band between coordinated equatorial ligands and the nonbonding or antibonding molecular orbitals of the UO_2^{2+} cation.[29]

We observe that UO_2^{2+} emission can be systematically influenced when different aromatic carboxylate and TPY ligands are used (Figure 9a−d). This is consistent with many other studies including that by Severance and co-workers, who noted shifts in uranyl emission as a function of pyridyl and pyrazine carboxylates.[51] To explain these shifts, we measured the peak positions of **1**−**4** and calculated the difference between the peak 1 energy values to each superimposed spectra. These values can be found in the Supporting Information (Tables S1 and S2). When TPY and Cl-TPY are kept constant, with changes between the TDC and BDC linkers (Figure 9a,d), an overall blue shift of −250 to −120 cm^{-1} of **1**, **3** and **2**, **4** is observed. Interestingly, the blue shift for **1** and **3** (Figure 9b) is more pronounced than that for **2** and **4** (Figure 9d) by −120 cm^{-1}, suggesting that the presence of chlorine has an influence on the observed spectra. On the other hand, when TPY and Cl-TPY are changed, keeping TDC and BDC constant (Figure 9a,c), the emission shifts are varied. A comparison of **3** and **4** (Figure 9c) using BDC shows a blue shift of −40 cm^{-1}, which seems to indicate that only chlorine has an influence on the observed shift. However, when **1** and **2** are compared using TDC (Figure 9a), a red shift of +80 cm^{-1} is shown. We speculate that this may be due to the presence of sulfur, which seems to counteract the effects of chlorine, with sulfur having a larger influence on the observed shifts. From our observations, we note that the presence of TDC and perhaps the chlorine of Cl-TPY influence the spectral shifts of uranyl TPY and Cl-TPY compounds. Like the emission spectra, the UV−vis diffuse-reflectance spectra (see Figure S13 in the Supporting Information) also show blue and red shifts for **1**−**4** compared to each other and uranyl acetate. It is unclear how the heteroatoms in these ligands affect the energy levels of the uranyl molecular orbitals. As such, a theoretical investigation to explain these phenomena is currently underway.

dx.doi.org/10.1021/ic3024698 | *Inorg. Chem.* 2013, 52, 2060−2069

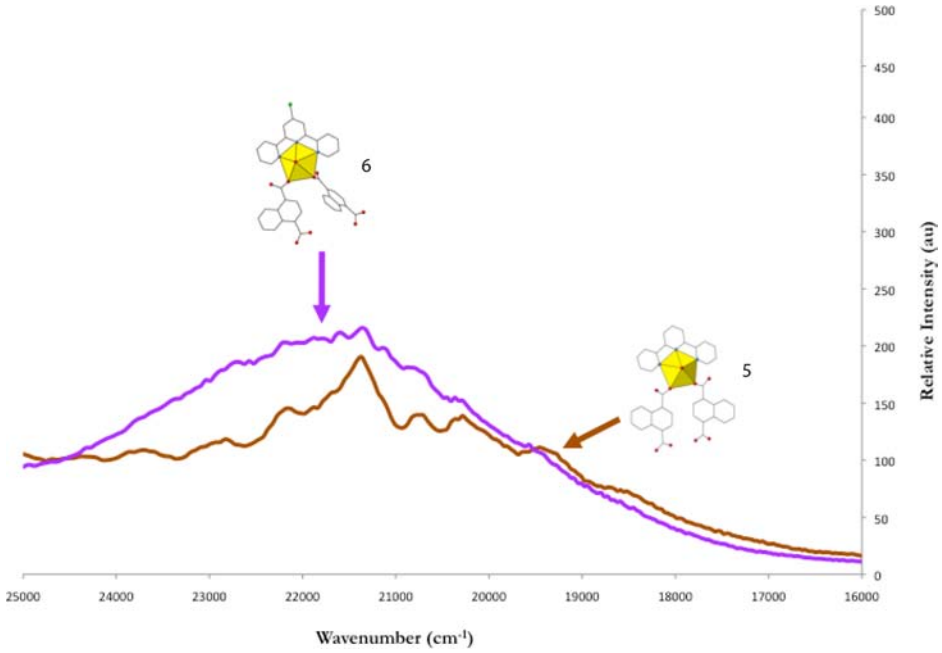

Figure 11. Solid-state emission spectra of **5** and **6** excited at 365 nm at room temperature.

To explore the potential for energy transfer between UO_2^{2+} and the ligands used in this study, the triplet energy levels for TPY, BDC, TDC, and NDC were obtained from measured values of gadolinium (Gd^{3+}) complexes described in the literature or determined via low-temperature phosphorescence spectra (see Figures S14 and S16 in the Supporting Information).[34,52] Phosphorescence measurements from Gd^{3+} complexes are a useful method to determine the triplet states of organic linkers because of the large energy gap (32000 cm^{-1}) between the $^8S_{7/2}$ ground state and the $^6P_{7/2}$ excited state of the Gd^{3+} ion.[53] As a result, the excited state of the Gd^{3+} ion cannot accept energy from the organic ligand, leading to a loss of energy by nonradiative decay and thereby allowing the ligand triplet energy to be measured. The energy levels of TDC, BDC, NDC, and TPY and the emissive uranyl state are compared (Figure 10).

In general, energy transfer requires two criteria that must be fulfilled. First, the position of the ligand triplet energy level should be slightly above the energy level of the emissive UO_2^{2+} ion (>1500 cm^{-1} is generally accepted to preclude efficient, thermally mediated back energy transfer). Second, the ligand itself should be at an appropriate transfer distance to the metal. Although the energy levels and distances of the ligands are indeed appropriate, the UV−vis diffuse-reflectance spectra (see Figure S13 in the Supporting Information) show that $\pi \rightarrow \pi^*$ absorption of the TPY ligands and aromatic carboxylates occurs in the same region as uranyl absorption, suggesting that we cannot indicate explicitly whether UO_2^{2+} sensitization has occurred.

Compared to the emission spectra of **1**−**4**, compounds **5** and **6** do not exhibit characteristic uranyl fluorescence (Figure 11), the absence of which suggests back energy transfer to NDC. In fact, of the ligands studied, the energy level of the NDC triplet is lowest compared to that of the excited UO_2^{2+} and may allow for a nonradiative decay from the uranyl to the ligand. In contrast, the triplet energy levels of TDC, BDC, and TPY are above the energy level of an excited UO_2^{2+}, which would, in turn, explain the observed uranyl emission in **1**−**4**. Lastly, the influence of π stacking on the fluorescence of uranyl CPs has been discussed[54] and may imply an additional contribution to the luminescence of **1**−**6** beyond the energy-transfer mechanisms presented thus far. That said, no obvious relationship between π stacking and luminescence is apparent in these compounds.

In summary, we have synthesized and characterized six novel uranyl terpyridine aromatic carboxylates using single-crystal XRD and PXRD and UV−vis and fluorescence spectroscopy. The coordination environment of the uranyl center with aromatic linkers and TPY ligands produces monomeric units that crystallize into molecular dimers (**1**, **2**, and **5**) or ladder-like chains (**3**, **4**, and **6**) under solvothermal conditions. Depending on the TPY ligands and coordinated aromatic carboxylates, we note that uranyl emission can be tuned, in which bathochromic and hypsochromic shifts are observed. At present, it is unclear what influence π stacking may have on uranyl emission, but future work to systematically explore such phenomena is currently in progress.

■ ASSOCIATED CONTENT

Ⓢ Supporting Information

X-ray crystallographic data in CIF format, PXRD patterns, ORTEP diagrams, and UV−vis spectra for **1**−**6**, tables of emission peak positions and spectral shifts, and phosphorescence spectra. This material is available free of charge via the Internet at http://pubs.acs.org.

■ AUTHOR INFORMATION

Corresponding Author

*E-mail: cahill@gwu.edu. Phone: (202) 994-6959.

Notes

The authors declare no competing financial interest.

■ ACKNOWLEDGMENTS

We gratefully acknowledge funding from the Materials Science of Actinides, an Energy Frontier Research Center, supported by the U.S. Department of Energy Office of Basic Energy Science

(Grant DE-SC0001089). We also thank Dr. Travis K. Holman (Georgetown University) for use of the Siemens X-ray diffractometer and Paula M. Cantos and Andrew T. Kerr (The George Washington University) for data collection of compound **4**.

REFERENCES

(1) Andrews, M. B.; Cahill, C. L. *Chem. Rev.* **2013**, DOI:10.1021/cr300202a.
(2) Rowland, C. E.; Cahill, C. L. *Inorg. Chem.* **2010**, *49*, 6716−6724.
(3) Thuery, P. *Cryst. Growth Des.* **2008**, *8*, 4132−4143.
(4) Lhoste, J.; Henry, N.; Roussel, P.; Loiseau, T.; Abraham, F. *Dalton Trans.* **2011**, *40*, 2422−2424.
(5) Pasquale, S.; Sattin, S.; Escudero-Adan, E. C.; Martinez-Belmonte, M.; de Mendoza, J. *Nat. Commun.* **2012**, *3*, 1−7.
(6) Mihalcea, I.; Henry, N.; Clavier, N.; Dacheux, N.; Loiseau, T. *Inorg. Chem.* **2011**, *50*, 6243−6249.
(7) Thuery, P. *CrystEngComm* **2012**, *14*, 6369−6373.
(8) Wang, K.-X.; Chen, J.-S. *Acc. Chem. Res.* **2011**, *44*, 531−540.
(9) Severance, R. C.; Smith, M. D.; zur Loye, H.-C. *Inorg. Chem.* **2011**, *50*, 7931−7933.
(10) Andrews, M. B.; Cahill, C. L. *Dalton Trans.* **2012**, *41*, 3911−3914.
(11) Deifel, N. P.; Cahill, C. L. *Cr. Chim.* **2010**, *13*, 747−754.
(12) Lhoste, J.; Henry, N.; Loiseau, T.; Guyot, Y.; Abraham, F. *Polyhedron* **2013**, DOI:10.1016/j.poly.2012.11.026.
(13) Charushnikova, I. A.; Den Auwer, C. *Russ. J. Coord. Chem.* **2004**, *30*, 511−519.
(14) Berthet, J.-C.; Nierlich, M.; Ephritikhine, M. *Dalton Trans.* **2004**, 2814−2821.
(15) Charushnikova, I.; Den Auwer, C. *Russ. J. Coord. Chem.* **2007**, *33*, 53−60.
(16) Allendorf, M. D.; Bauer, C. A.; Bhakta, R. K.; Houk, R. J. *Chem. Soc. Rev.* **2009**, *38*, 1330−1352.
(17) Cui, Y.; Yue, Y.; Qian, G.; Chen, B. *Chem. Rev.* **2012**, *112*, 1126−1162.
(18) de Lill, D. T.; de Bettencourt-Dias, A.; Cahill, C. L. *Inorg. Chem.* **2007**, *46*, 3960−3965.
(19) de Lill, D. T.; Gunning, N. S.; Cahill, C. L. *Inorg. Chem.* **2004**, *44*, 258−266.
(20) de Bettencourt-Dias, A. *Dalton Trans.* **2007**, 2229−2241.
(21) Eliseeva, S. V.; Bunzli, J.-C. G. *Chem. Soc. Rev.* **2010**, *39*, 189−227.
(22) Huang, W.; Wu, D.; Zhou, P.; Yan, W.; Guo, D.; Duan, C.; Meng, Q. *Cryst. Growth Des.* **2009**, *9*, 1361−1369.
(23) Sun, Y. G.; Jiang, B.; Cui, T. F.; Xiong, G.; Smet, P. F.; Ding, F.; Gao, E. J.; Lv, T. Y.; Van den Eeckhout, K.; Poelman, D.; Verpoort, F. *Dalton Trans.* **2011**, *40*, 11581−11590.
(24) Reineke, T. M.; Eddaoudi, M.; Fehr, M.; Kelley, D.; Yaghi, O. M. *J. Am. Chem. Soc.* **1999**, *121*, 1651−1657.
(25) Daiguebonne, C.; Kerbellec, N.; Guillou, O.; Bunzli, J. C.; Gumy, F.; Catala, L.; Mallah, T.; Audebrand, N.; Gerault, Y.; Bernot, K.; Calvez, G. *Inorg. Chem.* **2008**, *47*, 3700−3708.
(26) Yang, J.; Yue, Q.; Li, G.-D.; Cao, J.-J.; Li, G.-H.; Chen, J.-S. *Inorg. Chem.* **2006**, *45*, 2857−2865.
(27) Go, Y. B.; Wang, X.; Jacobson, A. J. *Inorg. Chem.* **2007**, *46*, 6594−6600.
(28) Severance, R. C.; Smith, M. D.; zur Loye, H. C. *Inorg. Chem.* **2011**, *50*, 7931−7933.
(29) Yu, Z.-T.; Liao, Z.-L.; Jiang, Y.-S.; Li, G.-H.; Chen, J.-S. *Chem.—Eur. J.* **2005**, *11*, 2642−2650.
(30) Liao, Z. L.; Li, G. D.; Bi, M. H.; Chen, J. S. *Inorg. Chem.* **2008**, *47*, 4844−4853.
(31) Xia, Y.; Wang, K.-X.; Chen, J.-S. *Inorg. Chem. Commun.* **2010**, *13*, 1542−1547.
(32) Jenniefer, S. J.; Muthiah, P. T. *Acta Crystallogr., Sect. C* **2011**, *67*, m69−m72.
(33) Mihalcea, I.; Henry, N.; Bousquet, T.; Volkringer, C.; Loiseau, T. *Cryst. Growth Des.* **2012**, *12*, 4641−4648.
(34) Murner, H. R.; Chassat, E.; Thummel, R. P.; Bunzli, J. C. G. *J. Chem. Soc., Dalton Trans.* **2000**, 2809−2816.
(35) Wu, Q.-R.; Wang, J.-J.; Hu, H.-M.; Shangguan, Y.-Q.; Fu, F.; Yang, M.-L.; Dong, F.-X.; Xue, G.-L. *Inorg. Chem. Commun.* **2011**, *14*, 484−488.
(36) Szabo, Z.; Toraishi, T.; Vallet, V.; Grenthe, I. *Coord. Chem. Rev.* **2006**, *250*, 784−815.
(37) Maher, K.; Bargar, J. R.; Brown, G. E. *Inorg. Chem.* **2013**, DOI: 10.1021/ic301686d.
(38) Grenthe, I.; Fuger, R. J. M.; Konings, R. J.; Lemire, A. B.; Muller, C.; Nguyen-Trun, H.; Wanner, H. *Chemical Thermodynamics of Uranium*; Wanner, H., Forest, I., Eds.; Nuclear Energy Agency, Organization for Economic Cooperation and Development: Issy-les-Moulineau, France, 2004.
(39) Wang, W.-D.; Bakac, A.; Espenson, J. H. *Inorg. Chem.* **1995**, *34*, 6034−6039.
(40) Nieweg, J. A.; Lemma, K.; Trewyn, B. G.; Lin, V. S. Y.; Bakac, A. *Inorg. Chem.* **2005**, *44*, 5641−5648.
(41) Frisch, M.; Cahill, C. L. *Dalton Trans.* **2005**, 1518−1523.
(42) Frisch, M.; Cahill, C. L. *Dalton Trans.* **2006**, 4679−4690.
(43) Sheldrick, G. *Acta Crystallogr., Sect. A* **2008**, *64*, 112−122.
(44) Farrugia, L. *J. Appl. Crystallogr.* **1999**, *32*, 837−838.
(45) Burns, P. C.; Ewing, R. C.; Hawthorne, F. C. *Can. Mineral.* **1997**, *35*, 1551−1570.
(46) Margoshes, M.; Fillwalk, F.; Fassel, V. A.; Rundle, R. E. *J. Chem. Phys.* **1954**, *22*, 381−382.
(47) Janiak, C. *J. Chem. Soc., Dalton Trans.* **2000**, 3885−3896.
(48) Denning, R. G. *J. Phys. Chem. A* **2007**, *111*, 4125−4143.
(49) Liu, G. K.; Vikhnin, V. S. *Chem. Phys. Lett.* **2007**, *437*, 56−60.
(50) Brachmann, A.; Geipel, G.; Bernhard, G.; Nitsche, H. *Radiochim. Acta* **2002**, *90*, 147−153.
(51) Severance, R. C.; Vaughn, S. A.; Smith, M. D.; zur Loye, H.-C. *Solid State Sci.* **2011**, *13*, 1344−1353.
(52) Hilder, M.; Junk, P. C.; Kynast, U. H.; Lezhnina, M. M. *J. Photochem. Photobiol. A* **2009**, *202*, 10−20.
(53) Teotonio, E. E. S.; Felinto, M. C. F. C.; Brito, H. F.; Malta, O. L.; Trindade, A. C.; Najjar, R.; Strek, W. *Inorg. Chim. Acta* **2004**, *357*, 451−460.
(54) Harrowfield, J. M.; Lugan, N.; Shahverdizadeh, G. H.; Soudi, A. A.; Thuéry, P. *Eur. J. Inorg. Chem.* **2006**, *2006*, 389−396.